

A Robust Adaptive Controller Design of Dual Arm Robot



Sung Hyun Han
Division of Mechanical and
Automation Eng., Kyungnam Univ.



Hideki Hashimoto
Institute of Industrial
Science Univ.

1. Introduction

Currently there are much advanced techniques that are suitable for servo control of a large class of nonlinear systems including robotic manipulators (P.C.V. Parks, 1966; Y.K. Choi et al., 1986; Y.M. Yoshhiko, 1995). Since the pioneering work of Dubowsky and DesForges (1979), the interest in adaptive control of robot manipulators has been growing steadily (T. C. Hasi, 1986; D. Koditschek, 1983; A. Koivo et al., 1983; S. Nicosia et al., 1984). This growth is largely due to the fact that adaptive control theory is particularly well-suited to robotic manipulators whose dynamic model is highly complex and may contain unknown parameters. However, implementation of these algorithms generally involves intensive numerical computations (J. J. Craig, 1988; H. Berghuis et al., 1993).

Current industrial approaches to the design of robot arm control systems treat each joint of the robot arm as a simple servomechanism. This approach models the time varying dynamics of a manipulator inadequately because it neglects the motion and configuration of the whole arm mechanism. The changes in the parameters of the controlled system are significant enough to render conventional feedback control strategies ineffective. This basic control system enables a manipulator to perform simple positioning tasks such as in the pick-and-place operation. However, joint controllers are severely limited in precise tracking of fast trajectories and sustaining desirable dynamic performance for variations of payload and parameter uncertainties (R. Ortega et al., 1989; P. Tomei, 1991). In many servo control applications the linear control scheme proves unsatisfactory, therefore, a need for nonlinear techniques is increasing.

Digital signal processors(DSP's) are special purpose microprocessors that are particularly suitable for intensive numerical computations involving sums and products of variables. Digital versions of most advanced control algorithms can be defined as sums and products of measured variables, thus can naturally be implemented by DSP's. DSPs allow straightforward implementation of advanced control algorithms that result in improved system control. Single and/or multiple axis control systems can be controlled by a single DSP. Adaptive and optimal multivariable control methods can track system parameter variations. Dual control, learning, neural networks, genetic algorithms and Fuzzy Logic control methodologies are all among the digital controllers implementable by a DSP(N. Sadegh et al., 1990; Z. Ma et al., 1995). In addition, DSP's are as fast in computation as most 32-bit microprocessors and yet at a fraction of their prices. These features make them a viable computational tool for digital implementation of advanced controllers. High performance DSPs with increased levels of integration for functional modules have become the dominant solution for digital control systems. Today's

DSPs with performance levels ranging from 5 to 5400 MIPS are on the market with price tags as low as \$3 (P. Bhatti et al., 1997; T. H. Akkermans et al., 2001). In order to develop a digital servo controller one must carefully consider the effect of the sample-and-hold operation, the sampling frequency, the computational delay, and that of the quantization error on the stability of a closed-loop system(S. A. Bortoff, 1994). Moreover, one must also consider the effect of disturbances on the transient variation of the tracking error as well as its steady-state value(F. Mehdian et al., 1995; S. H. Han et al., 1996).

This paper describes a new approach to the design of adaptive control system and real-time implementation using digital signal processors for robotic manipulators to achieve the improvement of speedness, repeating precision, and tracking performance at the joint and cartesian space. This paper is organized as follows : In Section II , the dynamic model of the robotic manipulator is derived. Section III derives adaptive control laws based on the model reference adaptive control theory using the improved Lyapunov second method. Section IV presents simulation and

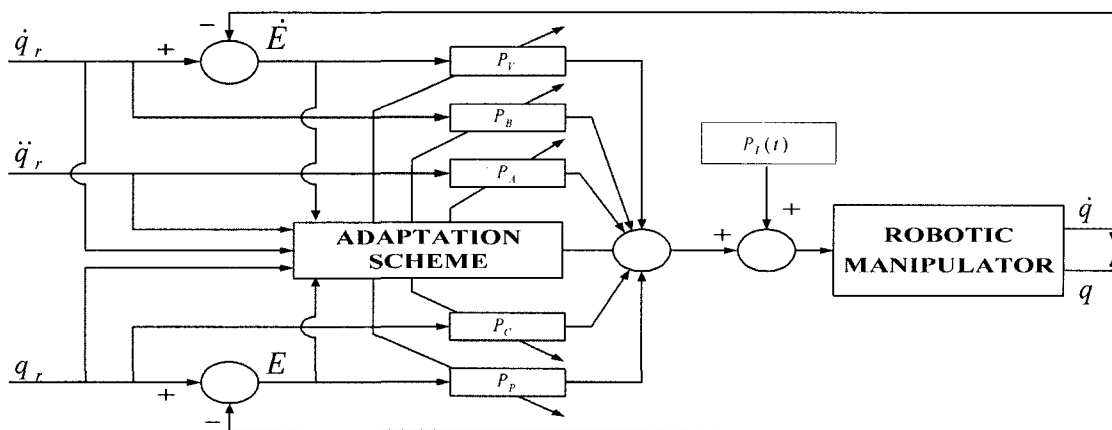


Fig 1. Adaptive control scheme of Robotic Manipulator with eight joint

experimental results obtained for a dual-arm robot. Finally, Section V discusses the findings and draws some conclusions.

2. System Modeling

The dynamic model of a manipulator-plus-payload is derived and the tracking control problem is stated in this section.

Let us consider a nonredundant joint robotic manipulator in which the $n \times 1$ generalized joint torque vector $\tau(t)$ is related to the $n \times 1$ generalized joint coordinate vector $q(t)$ by the following nonlinear dynamic equation of motion

$$D(q)\ddot{q} + N(q, \dot{q}) + G(q) = \tau(t) \quad (1)$$

where $D(q)$ is the $n \times n$ symmetric positive-definite inertia matrix, $N(q, \dot{q})$ is the $n \times 1$ coriolis and centrifugal torque vector, and $G(q)$ is the $n \times 1$ gravitational loading vector.

Equation (1) describes the manipulator dynamics without any payload. Now, let the $n \times 1$ vector X represent the end-effector position and orientation coordinates in a fixed task-related cartesian frame of reference. The cartesian position, velocity, and acceleration vectors of the end-effector are related to the joint variables by

$$\begin{aligned} X(t) &= \Phi(q) \\ \dot{X}(t) &= J(q)\dot{q}(t) \\ \ddot{X}(t) &= \dot{J}(q, \dot{q})\dot{q}(t) + J(q)\ddot{q}(t) \end{aligned} \quad (2)$$

where $\Phi(q)$ is the $n \times 1$ vector representing the forward kinematics and $J(q) = [\partial \Phi(q)/\partial q]$ is the $n \times n$ Jacobian matrix of the manipulator.

Let us now consider payload in the manipulator

dynamics. Suppose that the manipulator end-effector is firmly grasping a payload represented by the point mass ΔM_p . For the payload to move with acceleration $\ddot{X}(t)$ in the gravity field, the end-effector must apply the $n \times 1$ force vector $T(t)$ given by

$$T(t) = \Delta M_p [\ddot{X}(t) + g] \quad (3)$$

where g is the $n \times 1$ gravitational acceleration vector.

The end-effector requires the additional joint torque

$$\tau_f(t) = J(q)^T T(t) \quad (4)$$

where superscript T denotes transposition. Hence, the total joint torque vector can be obtained by combining equations (1) and (4) as

$$J(q)^T T(t) + D(q)\ddot{q} + N(q, \dot{q}) + G(q) = \tau(t) \quad (5)$$

Substituting equations (2) and (3) into equation (5) yields

$$\begin{aligned} \Delta M_p J(q)^T [J(q)\ddot{q} + \dot{J}(q, \dot{q})\dot{q} + g] \\ + D(q)\ddot{q} + N(q, \dot{q}) + G(q) = \tau(t) \end{aligned} \quad (6)$$

Equation (6) shows explicitly the effect of payload mass ΔM_p on the manipulator dynamics. This equation can be written as

$$\begin{aligned} [D(q) + \Delta M_p J(q)^T J(q)]\ddot{q} + [N(q, \dot{q}) \\ + \Delta M_p J(q)^T \dot{J}(q, \dot{q})\dot{q}] \\ + [G(q) + \Delta M_p J(q)^T g] = \tau(t) \end{aligned} \quad (7)$$

where the modified inertia matrix $[D(q) + \Delta M_p J(q)^T J(q)]$ is symmetric and positive-definite. Equation (7) constitutes a nonlinear mathematical model of the manipulator-plus-payload dynamics.

3. Adaptive Controller

The manipulator control problem is to develop a control scheme which ensures that the joint angle vector $q(t)$ tracks any desired reference trajectory $q_r(t)$, where $q_r(t)$ is an $n \times 1$ vector of arbitrary time functions. It is reasonable to assume that these functions are twice differentiable, that is, desired angular velocity $\dot{q}_r(t)$ and angular acceleration $\ddot{q}_r(t)$ exist and are directly available without requiring further differentiation of $q_r(t)$. It is desirable for the manipulator control system to achieve trajectory tracking irrespective of payload mass ΔM_p .

The controllers designed by the classical linear control scheme are effective in fine motion control of the manipulator in the neighborhood of a nominal operating point P_o . During the gross motion of the manipulator, operating point P_o and consequently the linearized model parameters vary substantially with time. Thus it is essential to adapt the gains of the feedforward, feedback, and PI controllers to varying operating points and payloads so as to ensure stability and trajectory tracking by the total control laws. The required adaptation laws are developed in this section. Fig. 1 represents the block diagram of adaptive control scheme for robotic manipulator.

Nonlinear dynamic equation (7) can be written as

$$\begin{aligned} \tau(t) = & D^*(\Delta M_p, q, \dot{q}) \ddot{q}(t) \\ & + N^*(\Delta M_p, q, \dot{q}) \dot{q}(t) \\ & + G^*(\Delta M_p, q, \dot{q}) q(t) \end{aligned} \quad (8)$$

where D^* , N^* and G^* are $n \times n$ matrices whose elements are highly nonlinear functions of $\Delta M_p, q$, and \dot{q} .

In order to cope with changes in operating point, the controller gains are varied with the change of external working condition.

This yields the adaptive control law

$$\begin{aligned} \tau(t) = & [P_A(t) \ddot{q}_r(t) + P_B(t) \dot{q}_r(t) \\ & + P_C(t) q_r(t)] + [P_V(t) \dot{E}(t) \\ & + P_P(t) E(t) + P_I(t)] \end{aligned} \quad (9)$$

where $P_A(t)$, $P_B(t)$, $P_C(t)$ are feedforward time-varying adaptive gains, and $P_p(t)$ and $P_v(t)$ are the feedback adaptive gains, and $P_I(t)$ is a time-varying control signal corresponding to the nominal operating point term, generated by a feedback controller driven by position tracking error $E(t)$ defined as $q_r(t) - q(t)$.

On applying adaptive control law (9) to nonlinear model (8) as shown in Fig. 1, the error differential equation can be obtained as

$$\begin{aligned} D^* \ddot{E}(t) + (N^* + P_V) \dot{E}(t) + (G^* + P_P) E(t) \\ = P_I(t) + (D^* - P_A) \ddot{q}_r(t) + (N^* - P_B) \dot{q}_r(t) \\ + (G^* - P_C) q_r(t) \end{aligned} \quad (10)$$

Defining the $2n \times 1$ position-velocity error vector $\delta(t) = [E(t), \dot{E}(t)]^T$, equation (10) can be written in the state-space form

$$\begin{aligned} \dot{\delta}(t) = & \begin{pmatrix} 0 & I_n \\ Z_1 & Z_2 \end{pmatrix} \delta(t) + \begin{pmatrix} 0 \\ Z_3 \end{pmatrix} q_r(t) \\ & + \begin{pmatrix} 0 \\ Z_4 \end{pmatrix} \dot{q}_r(t) + \begin{pmatrix} 0 \\ Z_5 \end{pmatrix} \ddot{q}_r(t) + \begin{pmatrix} 0 \\ Z_6 \end{pmatrix} \end{aligned} \quad (11)$$

where $Z_1 = -[D^*]^{-1} [G^* + P_P]$, $Z_2 = -[D^*]^{-1} [N^* + P_V]$, $Z_3 = [D^*]^{-1} [G^* - P_C]$, $Z_4 = [D^*]^{-1} [N^* - P_B]$, $Z_5 = [D^*]^{-1} [G^* - P_A]$ and $Z_6 = -[D^*]^{-1} [P_I]$

Equation (11) constitutes an adjustable system in the model reference adaptive control framework. We shall now define the reference model which embodies the desired performance of the manipulator in terms

of the tracking error $E(t)$. The desired performance is that each joint tracking error $E_i(t) = q_n(t) - q_i(t)$ be decoupled from the others and satisfy a second-order homogeneous differential equation of the form

$$\ddot{E}_i(t) + 2\xi_i\omega_i \dot{E}_i(t) + \omega_i^2 E_i(t) = 0 \quad (i = 1, \dots, n) \quad (12)$$

where ξ_i and ω_i are the damping ratio and the undamped natural frequency.

The desired performance of the control system is embodied in the definition of the stable reference model equation (12) as following vector equation (13).

$$\dot{\delta}_\gamma(t) = \begin{pmatrix} 0 & I_n \\ -S_1 & -S_2 \end{pmatrix} \delta_\gamma(t) \quad (13)$$

where $S_1 = \text{diag}(\omega_i^2)$ and $S_2 = \text{diag}(2\xi_i\omega_i)$ are constant $n \times n$ diagonal matrices, $\delta_\gamma(t) = [E_\gamma(t), \dot{E}_\gamma(t)]^T$ is the $2n \times 1$ vector of desired position and velocity errors, and the subscript ' γ ' denotes the reference model.

Because reference model is stable, equation (13) has Lyapunov function's solution R defined as following equation

$$RS + S^T R = -H \quad (14)$$

where H is symmetric positive definite matrix.

R is symmetric positive definite matrix defined as

$$\begin{bmatrix} R_1 & R_2 \\ R_2 & R_3 \end{bmatrix}.$$

We shall now state the adaptation laws which ensure that, for any reference trajectory $q_r(t)$, the state of the adjustable system, $\delta(t) = [E(t), \dot{E}(t)]^T$, approaches $\delta_r(t) = 0$ asymptotically. The controller adaptation laws will be derived using the direct Lyapunov

method-based model reference adaptive control technique. The adaptive control problem is to adjust the controller continuously so that, for any $q_r(t)$, the system state error $\delta(t)$ approaches asymptotically, i.e. $\delta(t) \rightarrow \delta_r(t)$ as $t \rightarrow \infty$.

Let the adaptation error be defined as $\varepsilon = [\delta_r(t) - \delta(t)]$, and then from equation (13), the error differential equation (11) can be defined as

$$\dot{\varepsilon} = \begin{pmatrix} 0 & I_n \\ -S_1 & -S_2 \end{pmatrix} \varepsilon + \begin{pmatrix} 0 & I_n \\ Z_1 - S_1 & Z_2 - S_2 \end{pmatrix} \begin{pmatrix} 0 \\ q_r \\ \dot{q}_r \\ \ddot{q}_r \end{pmatrix} + \begin{pmatrix} 0 \\ -Z_3 \end{pmatrix} q_r + \begin{pmatrix} 0 \\ -Z_4 \end{pmatrix} \dot{q}_r + \begin{pmatrix} 0 \\ -Z_5 \end{pmatrix} \ddot{q}_r + \begin{pmatrix} 0 \\ -Z_6 \end{pmatrix} \quad (15)$$

The controller adaptation laws shall be derived by ensuring the stability of error dynamics equation (15). To this end, let us define a scalar positive-definite Lyapunov function as

$$\begin{aligned} V = & \delta^T R \delta + \text{trace}\{[\Delta Z_1 - S_1]^T H_1 [\Delta Z_1 - S_1]\} \\ & + \text{trace}\{[\Delta Z_2 - S_2]^T H_2 [\Delta Z_2 - S_2]\} \\ & + \text{trace}\{[\Delta Z_3]^T H_3 [\Delta Z_3]\} \\ & + \text{trace}\{[\Delta Z_4]^T H_4 [\Delta Z_4]\} \\ & + \text{trace}\{[\Delta Z_5]^T H_5 [\Delta Z_5]\} \\ & + [\Delta Z_6^T H_6 \Delta Z_6] \end{aligned} \quad (16)$$

where $\Delta Z_1 = Z_1 - Z_1^*$, $\Delta Z_2 = Z_2 - Z_2^*$, $\Delta Z_3 = Z_3 - Z_3^*$, $\Delta Z_4 = Z_4 - Z_4^*$, $\Delta Z_5 = Z_5 - Z_5^*$, $\Delta Z_6 = Z_6 - Z_6^*$ and R is the solution of the Lyapunov equation for the reference model, $[H_1, \dots, H_6]$ are arbitrary symmetric positive-definite constant $n \times n$ matrices, and the matrices $[H_1, \dots, H_6]$ are functions of time which will be specified later. Now, differencing V along error trajectory and simplifying the result, We obtain

$$\begin{aligned} \dot{V} = & -\delta^T H \delta + 2Z_1^T [Q + H_1 \Delta Z_1] - 2Z_1^{*T} H_1 \dot{Z}_1 \\ & + 2\text{trace}\{ [Z_2 - S_2]^T [-Q E^T + H_2 \Delta Z_2] - Z_2^{*T} H_2 \Delta \dot{Z}_2 \} \\ & + 2\text{trace}\{ [Z_3 - S_3]^T [-Q E^T + H_3 \Delta Z_3] - Z_3^{*T} H_3 \Delta \dot{Z}_3 \} \\ & + 2\text{trace}\{ Z_4^T [Q q_r^T + H_4 \Delta Z_4] - Z_4^{*T} H_4 \Delta \dot{Z}_4 \} \\ & + 2\text{trace}\{ Z_5^T [Q \dot{q}_r^T + H_5 \Delta Z_5] - Z_5^{*T} H_5 \Delta \dot{Z}_5 \} \\ & + 2\text{trace}\{ Z_6^T [Q \ddot{q}_r^T + H_6 \Delta Z_6] - Z_6^{*T} H_6 \Delta \dot{Z}_6 \} \end{aligned} \quad (17)$$

where $\Delta Z_i = Z_i - Z_i^*$ and H_i is given by the Lyapunov equation (14) and

$$\begin{aligned} Q = & -[R_2, R_3] \delta = [R_2, R_3] \varepsilon \\ = & R_2 E + R_3 \dot{E} \end{aligned} \quad (18)$$

noting that $\varepsilon_m = 0$ and $\delta = -\varepsilon$. Now, for the adaptation error $f(t)$ to vanish asymptotically, i.e., for $\varepsilon(t) - \varepsilon_m(t)$, the function \dot{V} must be negative-definite in δ .

For this purpose, we set

$$\begin{aligned} Q + H_1 \dot{Z}_1 - H_1 \dot{Z}_1^* &= 0 \\ -Q E^T + H_2 \dot{Z}_2 - H_2 \dot{Z}_2^* &= 0 \\ -Q \dot{E}^T + H_3 \dot{Z}_3 - H_3 \dot{Z}_3^* &= 0 \\ Q q_r^T + H_4 \dot{Z}_4 - H_4 \dot{Z}_4^* &= 0 \\ Q \dot{q}_r^T + H_5 \dot{Z}_5 - H_5 \dot{Z}_5^* &= 0 \\ Q \ddot{q}_r^T + H_6 \dot{Z}_6 - H_6 \dot{Z}_6^* &= 0 \end{aligned} \quad (19)$$

From the equation (19), We obtain

$$\begin{aligned} H_1 [\dot{Z}_1 - \dot{Z}_1^*] &= -Q \\ H_2 [\dot{Z}_2 - \dot{Z}_2^*] &= -Q E^T \\ H_3 [\dot{Z}_3 - \dot{Z}_3^*] &= -Q \dot{E}^T \\ H_4 [\dot{Z}_4 - \dot{Z}_4^*] &= -Q q_r^T \\ H_5 [\dot{Z}_5 - \dot{Z}_5^*] &= -Q \dot{q}_r^T \\ H_6 [\dot{Z}_6 - \dot{Z}_6^*] &= -Q \ddot{q}_r^T \end{aligned} \quad (20)$$

In the case of definition of equation (19) and (20), \dot{V} reduces to

$$\begin{aligned} \dot{V} = & -\delta^T H \delta + 2Z_1^{*T} Q - 2\text{tr}[Z_2^{*T} Q E^T] \\ & - 2\text{tr}[Z_3^{*T} Q \dot{E}^T] + 2\text{tr}[Z_4^{*T} Q q_r^T] \\ & + 2\text{tr}[Z_5^{*T} Q \dot{q}_r^T] + 2\text{tr}[Z_6^{*T} Q \ddot{q}_r^T] \end{aligned} \quad (21)$$

Now, let us choose Z_1^*, \dots, Z_6^* as follows

$$\begin{aligned} Z_1^* &= -H_1^* Q \\ Z_2^* &= -H_1^* Q \\ Z_3^* &= -H_1^* Q \\ Z_4^* &= -H_4^* Q q_r^T \\ Z_5^* &= -H_5^* Q \dot{q}_r^T \\ Z_6^* &= -H_6^* Q \ddot{q}_r^T \end{aligned} \quad (22)$$

where H_1^*, \dots, H_6^* are symmetric positive semi-definite constant $n \times n$ matrices.

Equation (21) simplifies to

$$\begin{aligned} \dot{V} = & -\delta^T H \delta - 2Q^T H_1^* Q - 2(Q^T Q) E^T H_2^* E \\ & - 2(Q^T Q) \dot{E}^T H_3^* \dot{E} - 2(Q^T Q) q_r^T H_4^* q_r \\ & - 2(Q^T Q) \dot{q}_r^T H_5^* \dot{q}_r - 2(Q^T Q) \ddot{q}_r^T H_6^* \ddot{q}_r \end{aligned} \quad (23)$$

which is a negative definite function of δ in view of the positive semi-definiteness of H_1^*, \dots, H_6^* . Consequently, the error differential equation (15) is asymptotically stable; implying that $\varepsilon(t) \rightarrow \varepsilon_m(t)$ (or $\delta(t) \rightarrow 0$) as $t \rightarrow \infty$. Thus, from equations (20) and (22) adaptation laws are found to be

$$\begin{aligned} \dot{Z}_1 &= -H_1^{-1} Q - H_1^* Q \\ \dot{Z}_2 &= H_2^{-1} [Q E^T] + H_2^* \frac{d}{dt} [Q E^T] \\ \dot{Z}_3 &= H_3^{-1} [Q \dot{E}^T] + H_3^* \frac{d}{dt} [Q \dot{E}^T] \\ \dot{Z}_4 &= -H_4^{-1} [Q q_r^T] - H_4^* \frac{d}{dt} [Q q_r^T] \\ \dot{Z}_5 &= -H_5^{-1} [Q \dot{q}_r^T] - H_5^* \frac{d}{dt} [Q \dot{q}_r^T] \\ \dot{Z}_6 &= -H_6^{-1} [Q \ddot{q}_r^T] - H_6^* \frac{d}{dt} [Q \ddot{q}_r^T] \end{aligned} \quad (24)$$

Now, it is assumed that the relative change of the robot model matrices in each sampling interval is much smaller than that of the controller gains.

This implies that the robot model parameters D^* , N^* , and G^* can be treated as unknown and slowly time-varying compared with the controller gains.

This assumption is justifiable in practice since the robot model changes noticeably in the (50 msec) time-scale during rapid motion; whereas the controller gains can change significantly in the (10 msec) time-scale of the sampling interval. Hence there is typically two orders-of-magnitude difference between the controller and the robot time-scales. the adaptive controller continues to perform remarkably well. From the above assumption, Z_i can be derived as following

$$\begin{aligned}
\dot{Z}_1 &\approx -[D^*]^{-1} \dot{P}_l \\
\dot{Z}_2 &\approx [D^*]^{-1} \dot{P}_p^T \\
\dot{Z}_3 &\approx [D^*]^{-1} \dot{P}_v^T \\
\dot{Z}_4 &\approx -[D^*]^{-1} \dot{G} \\
\dot{Z}_5 &\approx -[D^*]^{-1} \dot{N} \\
\dot{Z}_6 &\approx -[D^*]^{-1} \dot{D}
\end{aligned} \tag{25}$$

In order to make the controller adaptation laws independent of the robot matrix, D^* , the H_i matrices in equations (23) are chosen as

$$\begin{aligned}
H_1 &= \lambda_1^{-1} D^* \\
H_2 &= p_1^{-1} D^* \\
H_3 &= \nu_1^{-1} D^* \\
H_4 &= c_1^{-1} D^* \\
H_5 &= b_1^{-1} D^* \\
H_6 &= a_1^{-1} D^*
\end{aligned} \tag{26}$$

where $\lambda_1, p_1, \nu_1, c_1, b_1$ and a_1 are positive scalars. And the H^* matrices in equation (24) are chosen as

$$\begin{aligned}
H_1^* &= \lambda_2 [D^*]^{-1} \\
H_2^* &= p_2 [D^*]^{-1} \\
H_3^* &= \nu_2 [D^*]^{-1} \\
H_4^* &= c_2 [D^*]^{-1} \\
H_5^* &= b_2 [D^*]^{-1} \\
H_6^* &= a_2 [D^*]^{-1}
\end{aligned} \tag{27}$$

where $\lambda_2, p_2, \nu_2, c_2, b_2$ and a_2 are zero or positive scalars.

Thus, from the equation (24) ~ (27), the gains of adaptive control law in equation (9) are defined as follows :

$$\begin{aligned}
P_A(t) &= a_1 [p_{a1} E + p_{a2} \dot{E}] [\ddot{q}_r]^T \\
&\quad + a_2 \int_0^t [p_{a1} E + p_{a2} \dot{E}] [\ddot{q}_r]^T dt + p_a(0)
\end{aligned} \tag{28}$$

$$\begin{aligned}
P_B(t) &= b_1 [p_{b1} E + p_{b2} \dot{E}] [\dot{q}_r]^T \\
&\quad + b_2 \int_0^t [p_{b1} E + p_{b2} \dot{E}] [\dot{q}_r]^T dt + p_b(0)
\end{aligned} \tag{29}$$

$$\begin{aligned}
P_C(t) &= c_1 [p_{c1} E + p_{c2} \dot{E}] [q_r]^T \\
&\quad + c_2 \int_0^t [p_{c1} E + p_{c2} \dot{E}] [q_r]^T dt + p_c(0)
\end{aligned} \tag{30}$$

$$P_I(t) = \lambda_2 [p_{i2} E] + \lambda_1 \int_0^t [p_{i1} E]^T dt + p_i(0) \tag{31}$$

$$\begin{aligned}
P_P(t) &= p_1 [p_{p1} E + p_{p2} \dot{E}] [E]^T \\
&\quad + p_2 \int_0^t [p_{p1} E + p_{p2} \dot{E}] [E]^T dt + p_p(0)
\end{aligned} \tag{32}$$

$$\begin{aligned}
P_V(t) &= \nu_1 [p_{v1} E + p_{v2} \dot{E}] [\dot{E}]^T \\
&\quad + \nu_2 \int_0^t [p_{v1} E + p_{v2} \dot{E}] [\dot{E}]^T dt + p_v(0)
\end{aligned} \tag{33}$$

where $[p_{p1}, p_{v1}, p_{c1}, p_{b1}, p_{a1}]$ and $[p_{p2}, p_{v2}, p_{c2}, p_{b2}, p_{a2}]$ are positive and zero/positive scalar adaptation gains, which are chosen by the designer to reflect the relative significance of position and velocity errors E and \dot{E} .

4. Simulation and Experiment

4.1 Simulation

This section represents the simulation results of the position and velocity control of a eight-link robotic manipulator by the proposed adaptive control

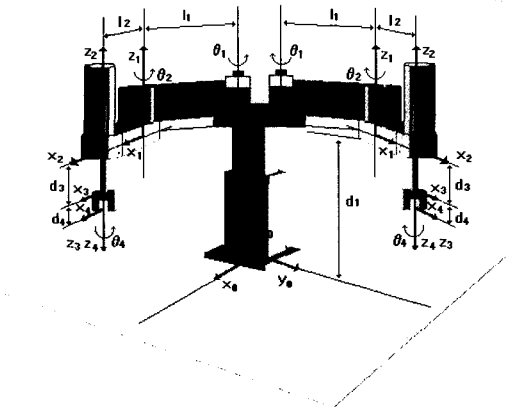


Fig. 2 Link coordinates of dual-arm robot

Table 1. Link parameters of robot.

Mass of link(kg)	Length of link(kg)	Inertia of link(kg)	Gear ratio of link
m1	l1	I1	r1
m2	l2	I2	r2
m3	l3	I3	r3
m4	l4	I4	r4
m5	l5	I5	r5
m6	l6	I6	r6
m7	l7	I7	r7
m8	l8	I8	r8

Table 2. Motor parameters of robot

Rotor inertia (kg m ²)	Torque constant (K m/a)	Back emf constant (V s/rad)	Amaturewinding resistance(ohms)
Jm1	Ka1	Kb1	Ra1
Jm2	Ka2	Kb2	Ra2
Jm3	Ka3	Kb3	Ra3
Jm4	Ka4	Kb4	Ra4
Jm5	Ka5	Kb5	Ra5
Jm6	Ka6	Kb6	Ra6
Jm7	Ka7	Kb7	Ra7
Jm8	Ka8	Kb8	Ra8

algorithm, as shown in Fig.2, and discusses the advantages of using joint controller based-on DSPs for motion control of a dual-arm robot. The adaptive scheme developed in this paper will be applied to the control of a dual-arm robot with eight axes. Fig.2 represents link coordinates of the dual-arm robot. Table 1 lists values of link parameters of the robot.

Table 2 lists motor parameters. Consider the dual-arm robot with the end-effector grasping a payload of mass ΔM_p . The emulation set-up consists of a TMS 320 evm DSP board and a Pentium III personal computer (PC). The TMS320 evm card is an application development tool which is based on the TI's TMS 320C80 floating-point DSP chip with 50ns instruction cycle time. The adaptive control algorithm is loaded into the DSP board, while the manipulator, the drive system, and the command generator are simulated in the host computer in C language. The communication between the PC and the DSP board is done via interrupts. These interrupts are managed by an operating system called A shell which is an extension of Windows9x. It is assumed that drive systems are ideal, that is, the actuators are permanent magnet DC motors which provide torques proportional to actuator currents, and that the PWM inverters are able to generate the equivalent of their inputs.

In all simulations the load is assumed to be unknown. The adaptive control algorithm given in equation (10) and parameter adaptation rules (28) ~ (33) as are used for the motion control of robot. The parameters associated with adaptation gains are selected by hand turning and iteration as $\lambda_1 = 0.5$, $\lambda_2 = 0.02$, $a_1 = 0.2$, $a_2 = 0.3$, $b_1 = 0.01$, $b_2 = 0.3$, $c_1 = 0.05$, $c_2 = 0.1$, $P_1 = 10$, $P_2 = 20$, $u_1 = 0.1$, $u_2 = 10$, $P_{a1} = 10^{-5}$, $P_{a2} = 10^{-4}$, $P_{b1} = 20$, $P_{b2} = 30$, $P_{c1} = 10$, $P_{c2} = 15$, $P_{P1} = 0.5$, $P_{P2} = 0.4$, $P_{\rho1} = 0.01$ and $P_{\rho2} = 0.05$.

It is assumed that $\omega_1 = \omega_2 = 10rad/sec$, $\xi_1 = \xi_2 = 1$,

and $S_1 = 80I$, $S_2 = 25I$ in the reference model. The sampling time is set as 0.001 sec. Simulations are performed to evaluate the position and velocity control of each joint under the condition of payload variation, inertia parameter uncertainty, and reference trajectory variation. Control performance for the reference trajectory variation is tested for four different position reference trajectories C and velocity reference trajectories D for each joint. As can be seen in Figs. 3 to 6, position reference trajectories C and velocity reference trajectory D consist of four different trajectories for joints 1, 2, 3, and 4.

The performance of DSP-based adaptive controller is evaluated in tracking errors of the position and velocity for the four joints.

The results of trajectory tracking of each joint in the different position cases are shown in Fig.'s 3~6. Fig. 3 shows results of angular position trajectory tracking and parameter uncertainties(6%) for each joint with a 4 kg payload and parameter uncertainties(6%) for reference trajectory C. Fig. 4 shows position trajectory tracking error for each joint with a 4 kg payload and parameter uncertainties(6%) As can be seen from these results, the DSP-based adaptive controller

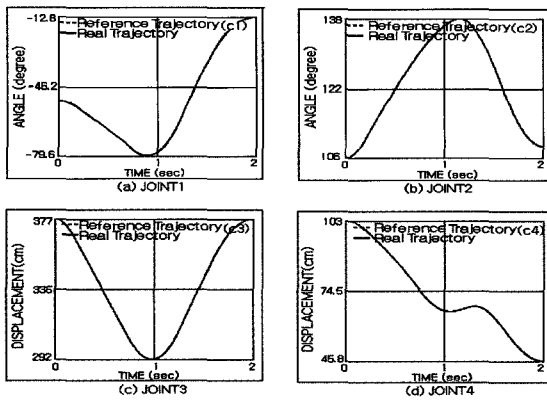


Fig. 3 (a)-(d) Position tracking performance of each joint with 4kg payload and inertia parameter uncertainty(6%) for reference trajectory C.

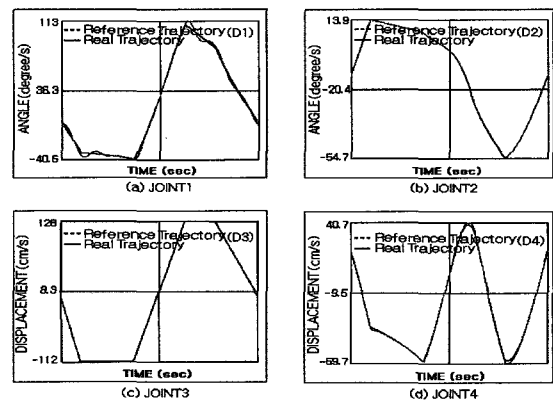


Fig. 5 (a)-(d) Velocity tracking performance of each joint with 4kg payload and inertia parameter uncertainty (6%) for reference trajectory D.

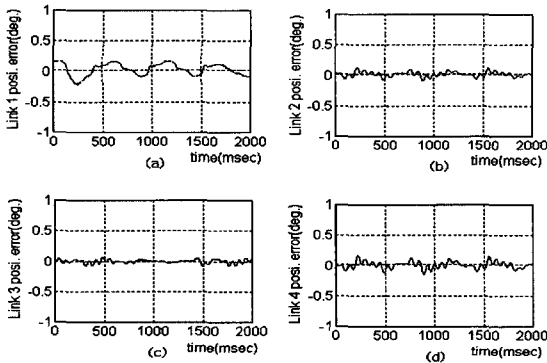


Fig. 4 (a)-(d) Position tracking error of each joint with 4kg payload and inertia parameter uncertainty (6%) for reference trajectory C.

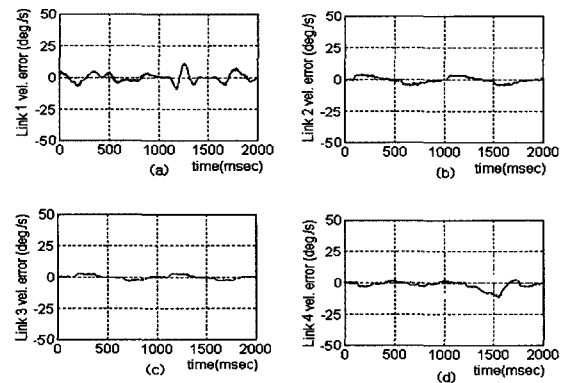


Fig. 6 (a)-(d) Velocity tracking error of each joint with 4kg payload and inertia parameter uncertainty(6%) for reference trajectory D.

represents extremely good performance with very small tracking error and fast adaptation response under the payload and parameter uncertainties.

Fig. 5. shows results of angular velocity tracking at each joint with payload(4 kg), parameter uncertainties(6%), for the reference trajectory D. Fig. 6 shows results of angular velocity tracking error at each joint with payload(4 kg), parameter uncertainties(6%) for reference trajectory D. As can be seen from Fig.'s 5 and 6, the proposed adaptive controller represents good performance in the position

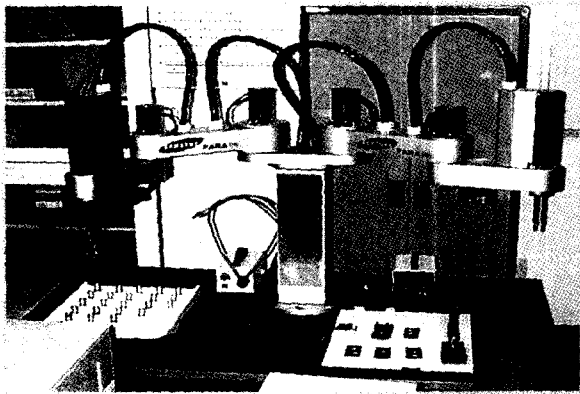


Fig. 7 Experimental set-up

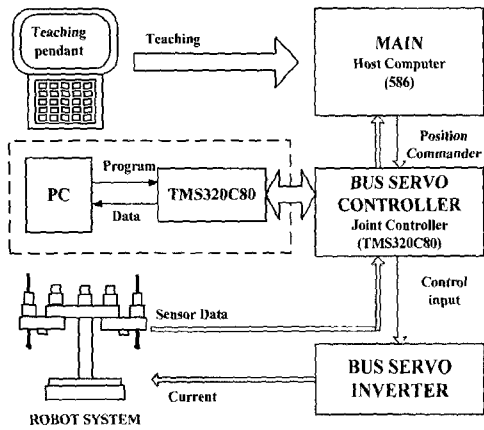


Fig. 8 The block diagram of the interface between the PC, DSP, and dual-arm robot.

and velocity at each joint for payload variation, inertia parameter uncertainty, and the change of reference trajectory. These simulation results illustrate that this DSP-based adaptive controller is very robust and suitable to real-time control due to its fast adaptation and simple structure

4.2 Experiment

The performance test of the proposed adaptive controller has been performed for the dual-arm robot at the joint space and cartesian space. At the cartesian space, it has been tested for the peg-in-hole tasks,

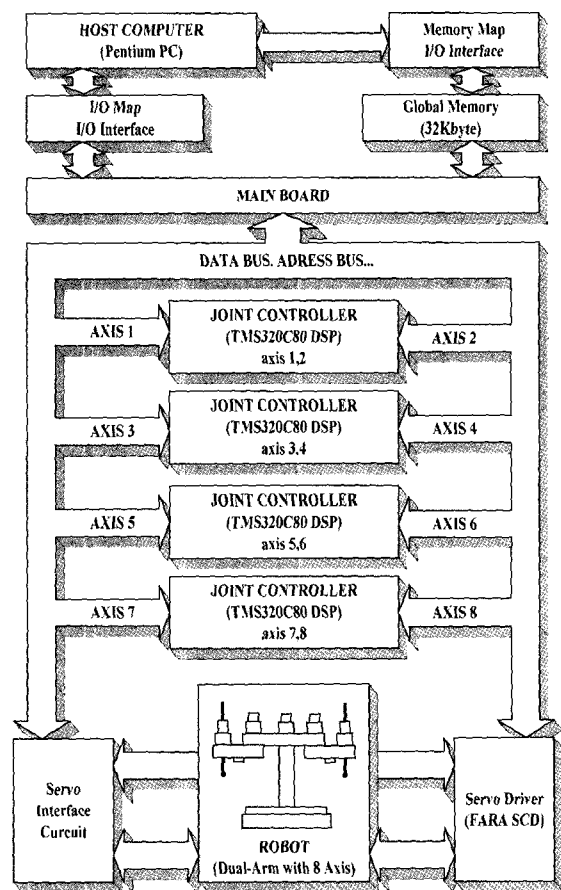


Fig. 9 The schematic diagram control system of dual-arm robot.

repeating precision tasks, and trajectory tracking for B-shaped reference trajectory. At the joint space, it has been tested for the trajectory tracking of angular position and velocity for a dual-arm robot made in Samsung Electronics Company in Korea. Fig. 7 represents the experimental set-up equipment. To implement the proposed adaptive controller, we used our own developed TMS320C80 assembler software. Also, the TMS320C80 emulator has been used in experimental set-up. At each joint of a dual-arm robot, a harmonic drive(with gear reduction ratio of 100 : 1 for joint 1 and 80 : 1 for joint 2) has been used to transfer power from the motor, which has a resolver attached to its shaft for sensing angular velocity with a resolution of 8096(pulses/rev). Fig. 8 represents the schematic diagram of control system of dual-arm robot. And Fig. 9 represents the block diagram of the interface between the PC, DSP, and dual-arm robot.

The performance test in the joint space is performed to evaluate the position and velocity control performance of the four joints under the condition of payload variation, inertia parameter uncertainty, and change of reference trajectory.

Fig.10 represents the B-shaped reference trajectory

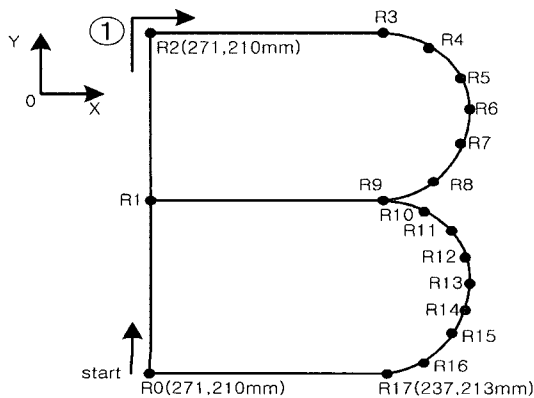


Fig. 10 The B shaped reference trajectory in the cartesian space.

in the cartesian space. Fig. 11 shows the experimental results of the position and velocity control at the first joint with payload 4 kg and the change of reference trajectory. Fig. 12 shows the experimental results for the position and velocity control at the second joint with 4 kg payload. Fig.'s 13 and 14 show the experimental results for the position and velocity control of the PID controller with 4 kg payload. As can be seen from these results, the DSP-based adaptive controller shows extremely good control performance with some external disturbances. It is illustrated that this control scheme shows better control performance than the

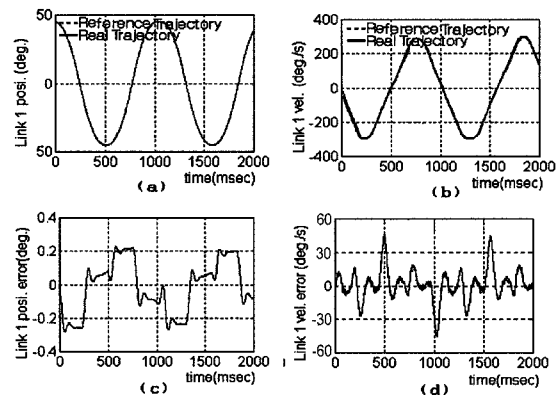


Fig. 11 (a)-(d) Experimental results for the position and velocity tracking of adaptive controller at the first joint with 4kg payload.

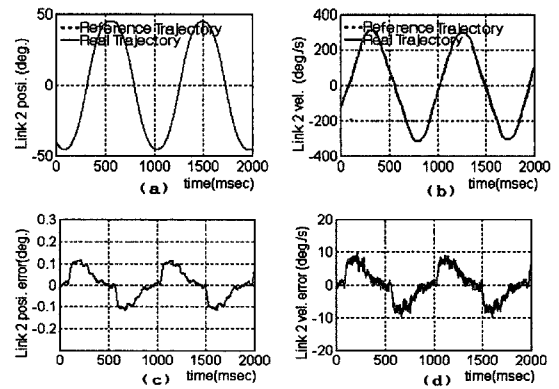


Fig. 12 (a)-(d) Experimental results for the position and velocity tracking of adaptive controller at the second joint with 4kg payload.

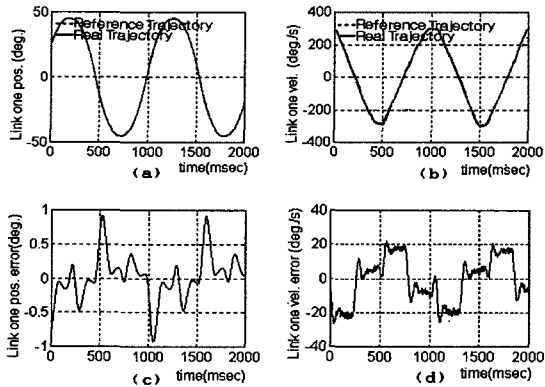


Fig. 13 (a)-(d) Experimental results of PID controller for the position and velocity tracking at the first joint with 4kg payload.

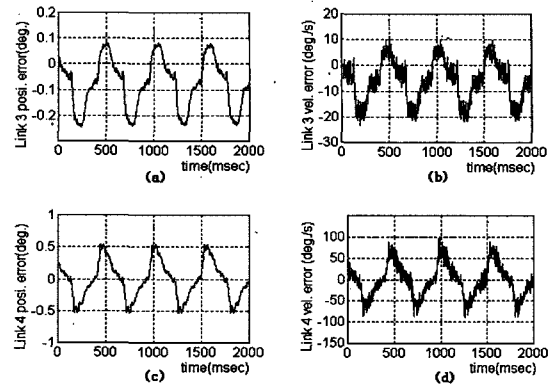


Fig. 16 (a)-(d) Experimental results for the position and velocity tracking of adaptive controller at the third joint and fourth joint with 4kg payload.

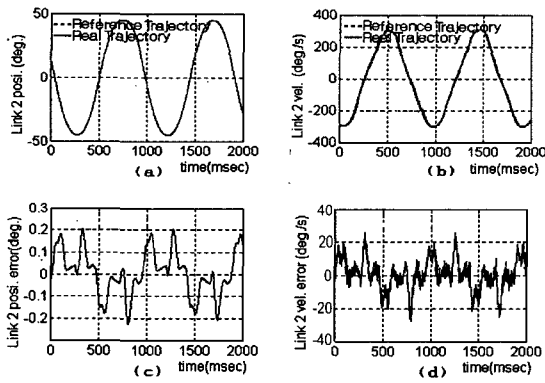


Fig. 14 (a)-(d) Experimental results of PID controller for the position and velocity tracking at the second joint with 4kg payload.

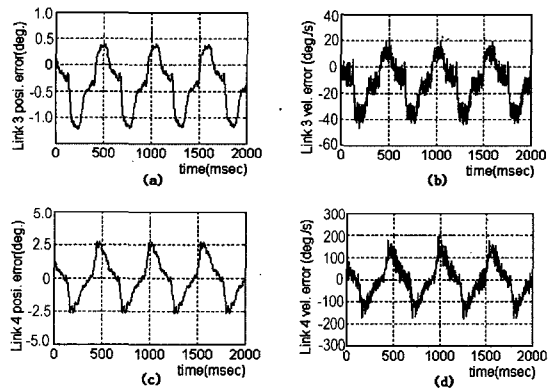


Fig. 17 (a)-(b) Experimental results for the position and velocity tracking of PID controller at the third joint and fourth joint with 4kg payload.

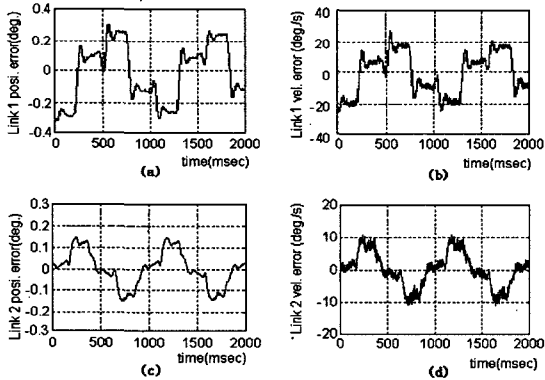


Fig. 15 (a)-(d) Experimental results for the position and velocity tracking of adaptive controller at the first joint and second joint with 4kg payload.

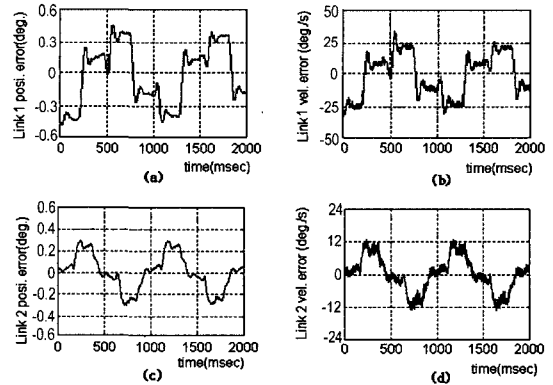


Fig. 18 (a)-(d) Experimental results for the position and velocity tracking of adaptive controller at the first joint and second joint with 6kg payload.

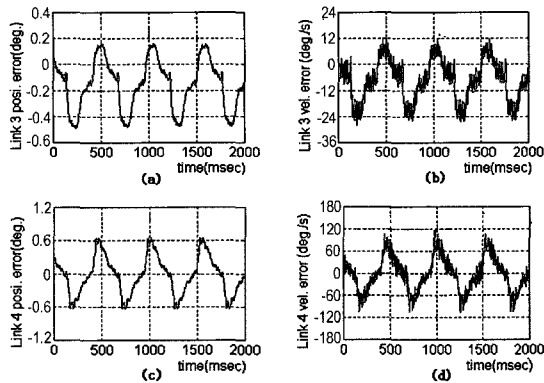


Fig. 19 (a)-(d) Experimental results for the position and velocity tracking of adaptive controller at the third joint and fourth joint with 6kg payload.

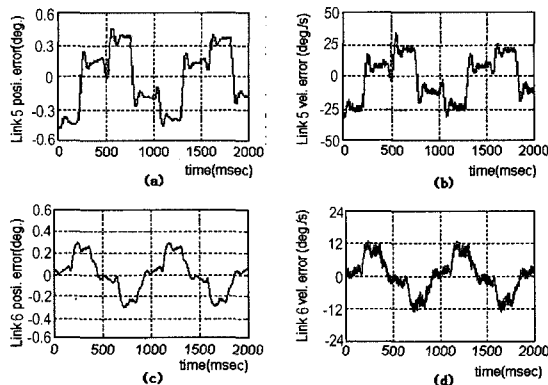


Fig. 20 (a)-(d) Experimental results for the position and velocity tracking of adaptive controller at the fifth and sixth joint with 6kg payload.

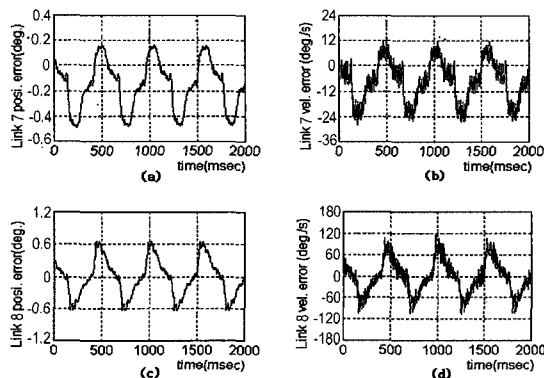


Fig. 21 (a)-(d) Experimental results for the position and velocity tracking of adaptive controller at the seventh joint and eighth joint with 6kg payload.

exiting PID controller, due to small tracking error and fast adaptation for disturbance.

Fig. 15 shows the experimental results of the position and velocity tracking performance at the first joint and second joint with 4 kg payload. Fig. 14 shows the experimental results of the position and velocity tracking performance at second joint with 4 kg payload. From the Fig. 15, it is illustrated that the proposed DSP-based adaptive controller is very robust and has fast adaptation response to the tracking of the position and velocity at the first joint with external disturbances. Fig. 15 shows the experimental results for the position and velocity control at the first joint and second joint with 4 kg payload. Fig. 15(a) represents the position tracking error of the first joint with 4 kg payload. Fig. 15(b) represents the velocity tracking error of the first joint with 4 kg payload. Fig. 15(c) represents the position tracking error of the second joint. Fig. 15(d) represents the velocity tracking error of the second joint. Fig. 16 shows the experimental for the position and velocity control at the third joint and fourth joint with 4 kg payload. Fig. 16(a) shows the position tracking error of the third joint with 4 kg payload. Fig. 16(b) shows the velocity tracking error of the third joint with 4 kg payload. Fig. 16(c) shows the position tracking error of the fourth joint. Fig. 16(d) shows the velocity tracking error of the fourth joint. As can be seen from above experimental results, it has been illustrated that the proposed adaptive scheme is very robust to the external disturbance, and suitable to real-time control of complex nonlinear systems, such as robot systems.

5. Conclusions

A new adaptive digital control scheme is described in this paper using DSP(TMS320C80) for robotic

manipulators. The adaptation laws are derived from the direct adaptive technique using the improved Lyapunov second method. The simulation and experimental results show that the proposed DSP-adaptive controller is robust to the payload variation, inertia parameter uncertainty, and change of reference trajectory. This adaptive controller has been found to be suitable to the real-time control of robot system. A novel feature of the proposed scheme is the utilization of an adaptive feedforward controller, an adaptive feedback controller, and a PI type time-varying control signal to the nominal operating point which result in improved tracking performance. Another attractive feature of this control scheme is that, to generate the control action, it neither requires a complex mathematical model of the manipulator dynamics nor any knowledge of the manipulator parameters and payload. The control scheme uses only the information contained in the actual and reference trajectories which are directly available. Furthermore, the adaptation laws generate the controller gains by means of simple arithmetic operations. Hence, the calculation control action is extremely simple and fast. These features are suitable for implementation of on-line real-time control for robotic manipulators with a high sampling rate, particularly when all physical parameters of the manipulator cannot be measured accurately and the mass of the payload can vary substantially. The proposed DSP-based adaptive controllers have several advantages over the analog control and the micro-computer based control. This allows instructions and data to be simultaneously fetched for processing. Moreover, most of the DSP instructions, including multiplications, are performed in one instruction cycle. The DSP tremendously increase speed of the controller and reduce computational delay, which

allows for faster sampling operation. It is illustrated that DSPs can be used for the implementation of complex digital control algorithms, such as our adaptive control for robot systems.

• ACKNOWLEDGEMENT

This work is supported by the Kyungnam University Research Fund, 2003.

REFERENCES

1. P.C.V. Parks, July 1966, "Lyapunov Redesign of Model Reference Adaptive Control System," IEEE Trans. Auto. Contr., Vol. AC-11, No. 3, pp. 362~267.
2. Y.K. Choi, M.J. Chang, and Z. Bien, 1986, "An Adaptive Control Scheme for Robot Manipulators." IEEE Trans. Auto. Contr., Vol. 44, No. 4, pp. 1185~1191.
3. Y.M. Yoshhiko, June 1995, "Model Reference Adaptive Control for Nonlinear System with unknown Degrees," In the proceeding of American Control Conference, pp.2505~2514, Seattle.
4. S. Dubowsky, and D.T. DesForges, 1979, "The Application of Model Reference Adaptation Control to Robot Manipulators," ASME J. Dyn. Syst., Meas., Contr., Vol. 101, pp. 193~200.
5. T.C. Hasi, 1986, "Adaptive Control Scheme for Robot Manipulators-A Review." In Proceeding of the 1987 IEEE Conference on Robotics and Automation, San Fransisco, CA.
6. D. Koditschek, 1983, "Quadratic Lyapunov Functions for Mecanical Systems," Technical Report No. 8703, Yale University, New Haven, CT.
7. J. J. Craig, 1988, "Adaptive Control of Meduanical Manipulator," Addison-wesley.
8. H. Berghuis, R.Orbega, and H.Nijmeijer, 1993, "A Robust Adaptive Robot controller," IEEE Trans., Robotics and Automation, Vol. 9, No. 6, pp. 825~830.
9. A. Koivo and T. H. Guo, 1983, "Adaptive Linear

- Controller for Robot Manipulators." IEEE Transactions and Automatic Control, Vol. AC-28, pp. 162~171.
- 10 R. Ortega and M.W. Spong, 1989, "Adaptive Motion Control of Rigid Robots : A Tutorial," Automatica, Vol. 25, pp. 877~888.
 - 11 P. Tomei, Aug. 1991, "Adaptive PD Controller for Robot Manipulators," IEEE Trans. Robotics and Automation, Vol.7, No.4.
 12. S. Nicosia and P. Tomee, 1984, "Model Reference Adaptive Control Algorithm for Industrial Robots," Automatica, Vol. 20, No. 5, pp. 635~644.
 13. N. Sadegh and R. Horowitz, Aug. 1990, "An Exponentially Stable Adaptive Control Law for Robot Manipulators," IEEE Trans. Robotics and Automation, Vol. 9, No. 4.
 14. Z. Ma, J. shen, A. Hug, and K. Nakayama, October 1995, "Automatic optimum Order Assignment in Adaptive Filters," international conference on signal Processing Applications & Technology, Boston pp. 629~633.
 15. T. A. Lasky and T. C. Hsia, July 1994, "Application of a Digital Signal Processor in Compliant Control of an Industrial Manipulator," Proceedings of American Control Conference.
 16. K. Michael and P. Issa, June 1995, "Digital Signal Processor : A Control Element," In Proceedings of American Control Conference, Seattle, pp. 470~474.
 17. S. A. Bortoff, Feb. 1994, "Advanced Nonlinear Robotic Control Using Digital Signal Processing," IEEE Trans. Indust. Elect., Vol. 41, No. 1.
 18. F. Mehdian and M. Wirth, June 1995, "Adaptive Control of Robotic Manipulators Using DSPs," In Proceedings of American Control Conference, Seattle, pp.480~481.
 19. S. H. Han, J. Lee, D. Ahn, M. Lee, and K. Son, July 1996, "Implementation of Robust Adaptive Controller of Robotic Manipulator using DSPs," "In Proceedings of Eleventh International Conference on System engineering, Lasvegas, pp. 668~673.
 20. T. H. Akkermans and S. G. Stan, 2001, "Digital servo IC for optical disc drives", Contr. Eng. Pract., vol. 9, no. 11, pp. 1245~1253.
 21. P. Bhatti and B. Hannaford, 1997, "Single-chip velocity measurement system for incremental optical encoders", IEEE Trans. Contr. Syst. Techn., vol. 5, no. 6, pp. 654~661.